Nuclear Physics A512 (1990) 46-60
North-Holland

STRUCTURE OF ^{11}Li IN THE CLUSTER-ORBITAL SHELL MODEL FOR THE ^{9}Li+n+n SYSTEM

Y. TOSAKA and Y. SUZUKI[1,*]

Graduate School of Science and Technology, Niigata University,
[1] *Physics Department, Niigata University, Niigata 950-21, Japan*
and
Physics Department, University of Michigan, Ann Arbor, MI 48109, USA

Received 1 December 1989

Abstract: The properties of ^{11}Li are studied in detail in the cluster-orbital shell model assuming the structure of ^{9}Li+n+n. The interactions acting between the constituent particles are carefully determined consistently with available data. Large and flexible bases for the valence neutrons are represented as a superposition of gaussian functions. The anomalously large radius of ^{11}Li is nicely reproduced. The density distributions calculated clarify the picture of the neutron halo. The binding energy is, however, calculated to be 1-1.4 MeV short. A possible resolution of this point is discussed from the viewpoint of the di-neutron clustering. The quadrupole moment of ^{11}Li is predicted to be almost the same as that of ^{9}Li.

1. Introduction

The recent development in the experimental technique of using radioactive nuclear beams has brought a new possibility of studying properties of nuclei far from stability. The measurement of the so-called interaction cross section [1], for example, has led to the extraction of the sizes of p-shell nuclei and shown that all the neutron drip line nuclei have anomalously large radii. The nucleus ^{11}Li, among others, has attracted most attention as a typical example of the light drip line nuclei. The characteristic features of ^{11}Li include: (i) The two-neutron separation energy of ^{11}Li is only 200 keV. Note that if ^{11}Li is considered as a system of ^{9}Li+n+n no pair of the constituent particles forms a particle-stable state. (ii) The matter root mean square radius of ^{11}Li determined experimentally is 3.16 ± 0.11 fm [ref. [1]], which is much larger than the empirical value of $\sqrt{\frac{3}{5}}\, r_0 A^{1/3} \approx 2.1$ fm. (iii) The transverse momentum distribution [2] of the nucleons obtained from the inclusive reaction ^{11}Li+C$\rightarrow$ ^{9}Li+anything is interpreted as consisting of two gaussian components. The narrow momentum distribution seems to suggest the motion of the two valence nucleons in a wide spatial region. These correlated properties of ^{11}Li all seem to support the existence of the so-called neutron halo [3].

* Work supported in part by the Grant-in Aid for Scientific Research of the Ministry of Education, Science and Culture, 1988-1989, Japan and the US National Science Foundation.

Although an attempt to understand some of the anomalous properties of ^{11}Li has been undertaken in shell-model [4]) and Hartree-Fock approaches [5,6]), no consistent study has been done for understanding the structure of ^{11}Li. Focusing ourselves on the properties (i) and (ii) mentioned above we work out in this paper a model which we call the cluster-orbital shell model [7,8]) in order to understand the structure of ^{11}Li. The cluster-orbital shell model is proposed to deal with a system of several valence nucleons coupled to a core. It has several advantageous points: Single-particle orbits can be determined consistently with underlying potentials between the core and the valence nucleon, the effect of continuum spectrum for the single-particle state can be taken into account and no spurious center-of-mass motion is included no matter how highly the valence nucleons are excited. These merits of the model encourage us to apply it especially to the study of neutron-rich nuclei. The He isotopes have in fact been investigated with considerable success [7,8]).

We take up a model for ^{11}Li that two valence neutrons move around the nucleus ^{9}Li. The assumption of the ^{9}Li core may be justified from the systematics of the binding energy per particle and the matter root mean square radii of Li isotopes that show a rather smooth behavior up to ^{9}Li but a big change between ^{9}Li and ^{11}Li as a function of neutron number. In calculations which follow we describe ^{9}Li with the harmonic-oscillator shell-model wave function of the lowest configuration. The extent to which this description is reasonable is confirmed by calculating the ground state properties of ^{9}Li. The $0\hbar\omega$ wave function predicts the ^{9}Li magnetic moment as 3.79 nuclear magneton compared with the observed value of 3.44 n.m. [refs. [9,10])]. The matter root mean square radius of ^{9}Li is given by $\sqrt{\frac{17}{9}}\,b$, where $b = \sqrt{\hbar/m\omega}$ is the size parameter of the harmonic-oscillator functions. The experimental value of 2.32 ± 0.02 fm [ref. [1])] leads to $b = 1.69$ fm. With this choice of b the ^{9}Li quadrupole moment, given by $-b^2$, becomes -2.86 fm^2, which is close to the experimental value of $-2.53 \pm 0\ 09$ fm^2 [ref. [10])]. All of these comparisons thus indicate that the $0\hbar\omega$ simple configuration of ^{9}Li is a reasonable approximation to its ground-state wave function provided that b is chosen as 1.69 fm.

The contents of the paper are as follows. The cluster-orbital shell model for the ^{9}Li+n+n system is briefly introduced in sect. 2.1. Sects. 2.2 and 2.3 are concerned with the investigation of the pair wise constituent particle systems of ^{9}Li+n and n+n, respectively. Results of calculations for energy, size, and density distribution are given in sect. 3. Summary and discussion is given in sect. 4.

2. The model

2.1. THE CLUSTER-ORBITAL SHELL MODEL FOR THE SYSTEM OF ^{9}Li+n+n

The detail of the cluster-orbital shell model is explained in ref. [8]). The following is mainly for clarifying the notations needed in the later sections. The basic hamil-

tonian in our model is given by

$$H = H_c + \sum_{i=1}^{2} h_i + v_{12} + \frac{1}{10m} \boldsymbol{p}_1 \cdot \boldsymbol{p}_2 , \tag{1}$$

with

$$h_i = \frac{1}{2m} \boldsymbol{p}_i^2 + U_i . \tag{2}$$

The H_c is the core hamiltonian of ^{9}Li. The U is the interaction potential between ^{9}Li and the valence neutron and consists of central and spin-orbit components. Its detailed form will be discussed in sect. 2.2. The v_{12} denotes the interaction potential between the two valence neutrons and includes central, spin-orbit and tensor components. The $\boldsymbol{p}_j = -i\hbar\partial/\partial\boldsymbol{\xi}_j$ is the momentum conjugate to the radius vector coordinate $\boldsymbol{\xi}_j$ from the center-of-mass of the ^{9}Li core to the jth valence neutron,

$$\boldsymbol{\xi}_j = \sqrt{\tfrac{9}{10}} \left[\boldsymbol{r}_j - \tfrac{1}{9}(\boldsymbol{r}_3 + \boldsymbol{r}_4 + \cdots + \boldsymbol{r}_{11}) \right] \qquad (j = 1, 2) . \tag{3}$$

The last term of eq. (1) is needed because the coordinate system chosen is given by a non-orthogonal transformation from the original coordinate system $\boldsymbol{r}_i$.

The total wave function of the system is specified by the angular momenta of the two valence neutrons relative to the core, j_1 and j_2, and their resultant angular momentum J. The spin and parity of the ^{11}Li ground state is $\frac{3}{2}^-$ [ref. [10])] so that the ground-state wave function is given in terms of a superposition of various orbital functions

$$|j_1 j_2, J, \tfrac{3}{2}; \tfrac{3}{2}M\rangle = [[\psi_{j_1}(1) \times \psi_{j_2}(2)]_J \times \psi_{3/2}(^9\mathrm{Li})]_{3/2M} , \tag{4}$$

where $\psi_{3/2}$ (^{9}Li) denotes the properly antisymmetrized, normalized internal wave function of ^{9}Li with spin and parity $\frac{3}{2}^-$ and ψ_j the wave function of the valence neutron. See ref. [8]) for the proper normalization of the total wave function.

As the ^{9}Li+n system has no bound state, the radial part of ψ_j should be flexible enough to be able to describe extended spatial motion. We assume that it can be approximated with a finite sum of gaussian functions $\chi_l(a, \xi)$ over a parameter a, where

$$\chi_l(a, \xi) \equiv \langle \xi | al \rangle = \left[\frac{2^{l+2} a^{l+3/2}}{(2l+1)!!\, \pi^{1/2} b^3} \right]^{1/2} \left(\frac{\xi}{b} \right)^l \exp\left[-\frac{a}{2} \left(\frac{\xi}{b} \right)^2 \right] . \tag{5}$$

Here b is the length scale parameter chosen as 1.69 fm in accordance with the size parameter of the ^{9}Li wave function. The basic single-particle orbit that the valence neutron occupies is thus given by

$$|aljm\rangle = \chi_l(a, \xi)[\, Y_l(\hat{\boldsymbol{\xi}}) \times \chi_{1/2}]_{jm} . \tag{6}$$

Note that orbits of this type are not orthogonal to each other with respect to a, but this does not cause any trouble in numerical calculations.

The minimum requirement of the Pauli principle is taken into account in eq. (4) by imposing that the valence neutron orbit should be orthogonal to the orbits of the core neutrons, namely $|a=1\ l=0\ \frac{1}{2}m\rangle$ and $|a=1\ l=1\ \frac{3}{2}m\rangle$. The elimination of these states from the valence orbit can easily be done by acting with the projection operator P on the state of eq. (6), where

$$P=1-\sum_m |10\tfrac{1}{2}m\rangle\langle 10\tfrac{1}{2}m|-\sum_m |11\tfrac{3}{2}m\rangle\langle 11\tfrac{3}{2}m|\,. \tag{7}$$

It is understood that this elimination is done in the following. The antisymmetry of the two valence neutrons is also easily taken into account but the explicit inclusion of antisymmetrization between the core and valence nucleons is neglected. This is expected to be a good approximation [8]) especially when the valence orbits spread over a wide region.

The experimental energy of ^{11}Li relative to the threshold of ^{9}Li+n+n is -200 keV, which is expressed with the expectation value $\langle h_1+h_2+v_{12}\rangle\approx -200$ keV when the term $(1/10m)\boldsymbol{p}_1\cdot\boldsymbol{p}_2$ is neglected. The matrix element of h_i is estimated as $\langle h_i\rangle\gtrsim$ 810 keV from the binding energy data of ^{10}Li and ^{9}Li. The interaction matrix element of v_{12} should therefore be about -1.8 MeV, in order to be consistent with all the experimental binding energies of $^{9\text{-}11}$Li. On the other hand, the two-neutron system has no bound state but a virtual state at about 70 keV. If the relative kinetic energy of the two neutrons is denoted by t_{12}, we must satisfy the relation $\langle t_{12}+v_{12}\rangle\gtrsim 70$ keV. It is therefore crucial for our model to investigate whether or not the conditions $\langle h_i\rangle\gtrsim 810$ keV, $\langle v_{12}\rangle\lesssim -1.8$ MeV, and $\langle t_{12}+v_{12}\rangle\gtrsim 70$ keV are all met simultaneously.

2.2. THE ^{9}Li+n SYSTEM

The central part U^{c} of the potential U acting between ^{9}Li and the valence neutron is assumed to be given by the folding potential. When the two-nucleon central potential is expressed as

$$v_{12}=(W+BP_\sigma-HP_\tau-MP_\sigma P_\tau)\exp[-\rho(\boldsymbol{r}_1-\boldsymbol{r}_2)^2]\,, \tag{8}$$

with the spin and isospin exchange operators P_σ and P_τ, the resulting folding potential has the form

$$\begin{aligned} U^{\mathrm{c}}_{\alpha',\alpha,J}(\xi)\equiv{}&\langle[[\,Y_{l'}(\hat{\boldsymbol{\xi}})\times\chi_{1/2}]_{j'}\times\psi_{3/2}(^{9}\mathrm{Li})]_{JM}| \\ &\times\sum_{k=2}^{10} v_{1k}|[[\,Y_l(\hat{\boldsymbol{\xi}})\times\chi_{1/2}]_j\times\psi_{3/2}(^{9}\mathrm{Li})]_{JM}\rangle \\ ={}&\left[\frac{9}{4\lambda+9}\right]^{3/2}\exp\left[-\frac{5\lambda}{4\lambda+9}\left(\frac{\xi}{b}\right)^2\right]f_{\alpha',\alpha,J}\left(\frac{\xi}{b}\right), \end{aligned} \tag{9}$$

where $\lambda = 2\rho b^2$, α stands for a set of the indices (l, j) and

$$f_{\alpha',\alpha,J}(x) = \delta_{jj'}\delta_{ll'}\left[4W+2B-2H-M+(5W+2B-4H-2M)\right.$$
$$\left.\times\left(\frac{18-\lambda}{2(4\lambda+9)}+\frac{15\lambda^2}{(4\lambda+9)^2}x^2\right)\right]$$
$$+\delta_{ll'}B\begin{bmatrix} l & \frac{1}{2} & j \\ \frac{1}{2} & 1 & \frac{3}{2} \\ j' & \frac{3}{2} & J \end{bmatrix}\left(\frac{18-\lambda}{2(4\lambda+9)}+\frac{15\lambda^2}{(4\lambda+9)^2}x^2\right)$$
$$+(-1)^{J+1}W\frac{3\sqrt{2}\,\lambda^2}{(4\lambda+9)^2}\left[\frac{(2l+1)(2l'+1)(2j+1)(2j'+1)}{(2J+1)}\right]^{1/2}\langle l0l'0|20\rangle$$
$$\times U(ll'jj';2\tfrac{1}{2})U(jj'\tfrac{3}{2}\tfrac{3}{2};2J)x^2$$
$$+(-1)^{J+1}B\frac{4\sqrt{30}\,\lambda^2}{(4\lambda+9)^2}\left[\frac{(2l+1)(2l'+1)}{(2J+1)}\right]^{1/2}\langle l0l'0|20\rangle x^2\sum_{II'}(-1)^{I+I'}$$
$$\times U(l\tfrac{1}{2}J\tfrac{3}{2};jI)U(l'\tfrac{1}{2}J\tfrac{3}{2};j'I')U(ll'II';2J)\begin{bmatrix} \frac{3}{2} & \frac{1}{2} & 1 \\ \frac{1}{2} & \frac{3}{2} & 1 \\ I & I' & 2 \end{bmatrix}. \qquad (10)$$

Here the $R(3)$ Racah or U-coefficients and $9j$ coefficients are given in unitary form. Note that ξ is $\sqrt{\frac{9}{10}}$ times the physical distance between ^{9}Li and the valence neutron. Eq. (9) has been obtained with the use of the Bargmann transform technique [11].

The spin-orbit part U^{ls} of the potential U would be generated in a similar way from two-nucleon spin-orbit potential. But its calculation turns out to be quite tedious. We assume that U^{ls} is diagonal with respect to the index α and its form is proportional to the gradient of the ^{9}Li density $\rho(\xi)$, that is $U^{ls}(\xi)\propto (\boldsymbol{l}\cdot\boldsymbol{s})(1/\xi)(\mathrm{d}/\mathrm{d}\xi)\rho(\xi)$. The use of the density averaged over the z-component of the ^{9}Li spin leads to the form

$$U^{ls}_{\alpha,\alpha,J}(\xi) = U_0\tfrac{1}{2}[j(j+1)-l(l+1)-\tfrac{3}{4}]\left[1-\frac{25}{2}\left(\frac{\xi}{b}\right)^2\right]\exp\left[-\frac{5}{4}\left(\frac{\xi}{b}\right)^2\right]. \qquad (11)$$

Considering that the spacing between the spin-orbit partners ($j = l\pm\frac{1}{2}$) of neutron-rich nuclei is expected to be smaller than that of stable nuclei, we set U_0 to 1.5 MeV, which gives the $0p_{3/2}$–$0p_{1/2}$ splitting of 3.8 MeV in ^{9}Li.

As the spin-orbit potential is fixed we next tune the central potential to reproduce the ground state energy of ^{10}Li, 810 keV from ^{9}Li+n. We use the Hasegawa-Nagata (HN) no. 1 potential [12]) as the two-nucleon central potential of eq. (8). We have

tested various spins of the ^{10}Li ground state and found that the state with 1^+ becomes lowest in energy and the state with 2^+ is almost degenerate with the ground state. This is in agreement with the shell model calculation of ref. [13]). We note that if we increase the strength of the spin-orbit potential by a factor of 2 the state with 2^- comes down close to the ground state. The possibility that the ground state of ^{10}Li is 2^- was discussed in ref. [14]), but for this to occur we need a very strong spin-orbit potential. The $p_{1/2}$, $p_{3/2}$ and $f_{5/2}$ orbits only are possible for the valence neutron to make 1^+ from the coupling of ^{9}Li with $\frac{3}{2}^-$. Expressing the relative motion function between ^{9}Li and the neutron as a superposition of states of the type of eq. (6) we have minimized the relative motion hamiltonian, $-(\hbar^2/2m)\partial^2/\partial\xi^2 + U^c + U^{ls}$, for two cases: (1) $p_{1/2}$ orbit only, (2) $p_{1/2}$, $p_{3/2}$ and $f_{5/2}$ orbits are included. The adopted values of a are given in a geometric series as

$$a = 0.24 \times 10^{(i-1)/9} \qquad (i = 1, 2, \ldots, 10) \quad \text{for } p_{1/2},$$

$$a = 0.24 \times 10^{(i-1)/4} \qquad (i = 1, 2, \ldots, 5) \quad \text{for } p_{3/2} \text{ and } f_{5/2}.$$

Small values of a are included to give a good description of the relative motion wave functions up to about 10 fm. Multiplying by 1.034 the strength of the medium-range part of the HN potential reproduces the empirical energy of 810 keV, namely 802 keV in case (1) and 798 keV in case (2). Fig. 1 shows the diagonal parts of the potentials of U^c, U^{ls}, and $U^c + U^{ls} + \hbar^2 l(l+1)/2m\xi^2$ for the case $p_{1/2}$ ($l = 1, j = \frac{1}{2}$, $J = 1$). Also shown are the wave functions obtained in cases (1) and (2). The U^c has a longer tail than the Woods-Saxon potential with the empirical parameters. The total effective potential has a very broad peak with a height of about 1 MeV at 5 fm. The amplitude of the corresponding relative wave function is peaked inside the potential peak but is spread over a large distance.

2.3. THE n+n SYSTEM

We take into account central, spin-orbit and tensor potentials as the two-nucleon potential acting between the valence neutrons. The central potential is taken from the HN no. 1 potential with a slight modification of its strength described below. The strengths and ranges of the spin-orbit (G3RS) and tensor parts are given in ref. [12]).

The strength of the central potential is determined so as to reproduce the virtual state energy of the singlet S di-neutron system at about 70 keV. We have calculated the energy by expanding the relative wave function with gaussian functions $\exp[-\frac{1}{2}(r/a)^2]$. The adopted values of a are in unit of fm

$$a = 0.4 \times 17.5^{(i-1)/11} \qquad (i = 1, 2, \ldots, 12).$$

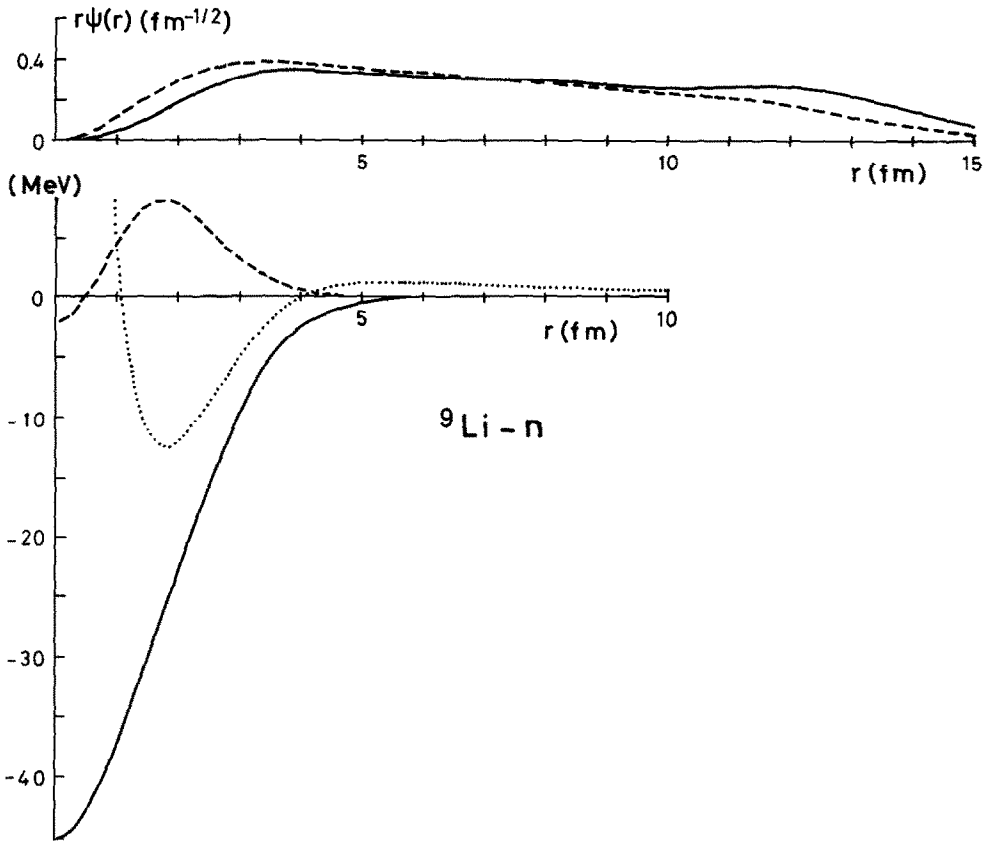

Fig. 1. The ^{9}Li–n potentials and their relative wave functions. The solid, dashed and dotted curves of the lower half figure denote the diagonal potentials of U^c, U^{ls}, and $U^c + U^{ls} + \hbar^2 l(l+1)/2m\xi^2$ in case of $l=1$, $j=\frac{1}{2}$, $J=1$, respectively. The solid and dashed curves of the upper half figure denote the wave functions obtained in cases (1) and (2) described in the text. The relative distance r is related to ξ of eq. (3) by $r=\sqrt{\frac{10}{9}}\,\xi$.

Multiplying by 0.91 the strength of the medium-range part of the HN no. 1 potential yields 76 keV for the virtual state energy. For the sake of comparison we also use the Volkov no. 2 potential [15]) which has no repulsion at short distance. This potential must be weakened by 21.5% to reproduce the virtual state energy when the Majorana exchange mixture is set to 0.62. Fig. 2 shows the wave function and central potential for each case. Although the two potentials are different in shape, the wave functions obtained are quite similar except for the region of short distance of less than 2 fm. It should be noted that small values of a are needed to describe such short distance behavior as obtained in the case of the HN potential. The expectation value of the central potential is about -1.7 MeV, which is very close to the value required in sect. 2.1.

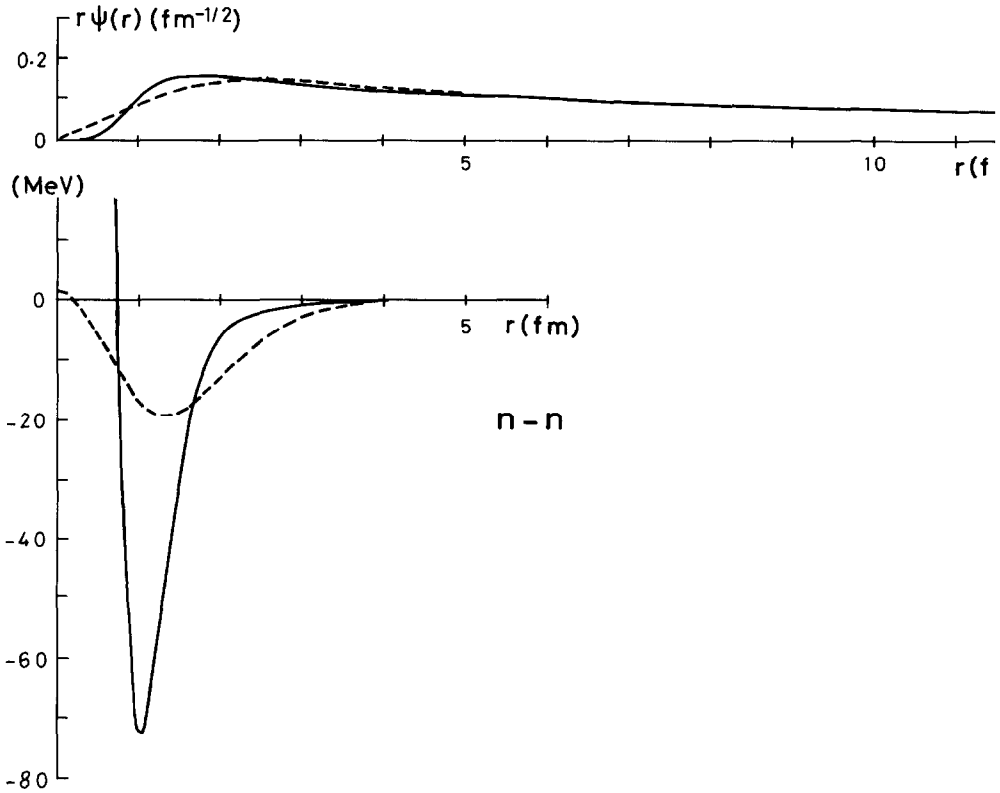

Fig. 2. The central part of the nn potential and the nn relative wave function. The solid and dashed curves of the lower half figure denote the HN no. 1 and Volkov no. 2 potentials which are adjusted to locate the virtual state at about 70 keV. The solid and dashed curves of the upper half figure denote the corresponding relative wave functions in the singlet S-channel.

3. Results of the calculation

3.1. ENERGY

The evaluation of the hamiltonian matrix elements is straightforward. Denoting the basis state as $|a_1 l_1 j_1\ a_2 l_2 j_2, J, \frac{3}{2}; \frac{3}{2}M\rangle$ from eqs. (4) and (6), we obtain

$$\begin{aligned}
&\langle a_1' l_1' j_1'\ a_2' l_2' j_2', J', \tfrac{3}{2}; \tfrac{3}{2}M|H|a_1 l_1 j_1\ a_2 l_2 j_2, J, \tfrac{3}{2}; \tfrac{3}{2}M\rangle \\
&\quad = \delta_{JJ'}\delta_{j_1 j_1'}\delta_{l_1 l_1'}\delta_{j_2 j_2'}\delta_{l_2 l_2'}\langle a_1' l_1'|a_1 l_1\rangle\langle a_2' l_2'|a_2 l_2\rangle E(^9\mathrm{Li}) \\
&\qquad + \sum_I U(j_1 j_2 \tfrac{3}{2}\tfrac{3}{2}; JI)\, U(j_1' j_2' \tfrac{3}{2}\tfrac{3}{2}; J'I) \\
&\qquad \times[(-1)^{j_1+j_2-J+j_1'+j_2'-J'}\delta_{j_2 j_2'}\delta_{l_2 l_2'}\langle a_2' l_2'|a_2 l_2\rangle\langle a_1' l_1'|h_{l_1' j_1', l_1 j_1, I}|a_1 l_1\rangle \\
&\qquad + \delta_{j_1 j_1'}\delta_{l_1 l_1'}\langle a_1' l_1'|a_1 l_1\rangle\langle a_2' l_2'|h_{l_2' j_2', l_2 j_2, I}|a_2 l_2\rangle] \\
&\qquad + \delta_{JJ'}\langle a_1' l_1' j_1' a_2' l_2' j_2'; JM|v_{12} + \frac{1}{10m}\boldsymbol{p}_1\cdot\boldsymbol{p}_2|a_1 l_1 j_1 a_2 l_2 j_2; JM\rangle\,,
\end{aligned}$$

where $E(^9\mathrm{Li}) \equiv \langle \psi_{3/2m}(^9\mathrm{Li}) | H_c | \psi_{3/2m}(^9\mathrm{Li}) \rangle$ is replaced with the observed energy of the ^{9}Li ground state, and $h_{l'j',lj,I}(\xi)$ is defined by

$$\langle Y_{lm}(\hat{\boldsymbol{\xi}}) | -\frac{\hbar^2}{2m}\frac{\partial^2}{\partial \boldsymbol{\xi}^2} | Y_{lm}(\hat{\boldsymbol{\xi}}) \rangle \delta_{jj'}\delta_{ll'} + U_{l'j',lj,I}(\xi).$$

Since the radial part of eq. (5) has a simple form, the matrix elements for two-nucleon interactions of gaussian radial dependence are reduced to the evaluation of integrals which can be analytically done.

Fig. 3 shows the energy of ^{11}Li relative to ^{9}Li as a function of a for the configuration of seniority 0, $|(alj)^2, 0, \frac{3}{2}; \frac{3}{2}M\rangle$ or $(alj)^2_{J=0}$ in short. It is seen that the $(ap_{1/2})^2_{J=0}$ state makes the energy lowest and is thus expected to be a dominant component in the ^{11}Li ground state. The energy of the $(ap_{1/2})^2_{J=0}$ configuration is rather flat for $a < 0.6$. This suggests that the valence neutron orbit spreads out to a large distance. The energies of the other configurations become rapidly high with increasing a.

We have successively extended the energy calculation to include larger bases in the following way:

(1) $(p_{1/2})^2_{J=0}$.
(2) $(p_{1/2})^2_{J=0}, (s_{1/2})^2_{J=0}, (d_{5/2})^2_{J=0}, (d_{3/2})^2_{J=0}$.
(3) $(p_{1/2})^2_{J=0}, (s_{1/2})^2_{J=0}, (d_{5/2})^2_{J=0}, (d_{3/2})^2_{J=0}, (p_{3/2})^2_{J=0}, (f_{7/2})^2_{J=0}, (f_{5/2})^2_{J=0}$.
(4) $(p_{1/2})^2_{J=0}, (s_{1/2})^2_{J=0}, (d_{5/2})^2_{J=0}, (d_{3/2})^2_{J=0}, (p_{3/2})^2_{J=0}, (f_{7/2})^2_{J=0}, (f_{5/2})^2_{J=0}$, $(g_{9/2})^2_{J=0}, (g_{7/2})^2_{J=0}$.

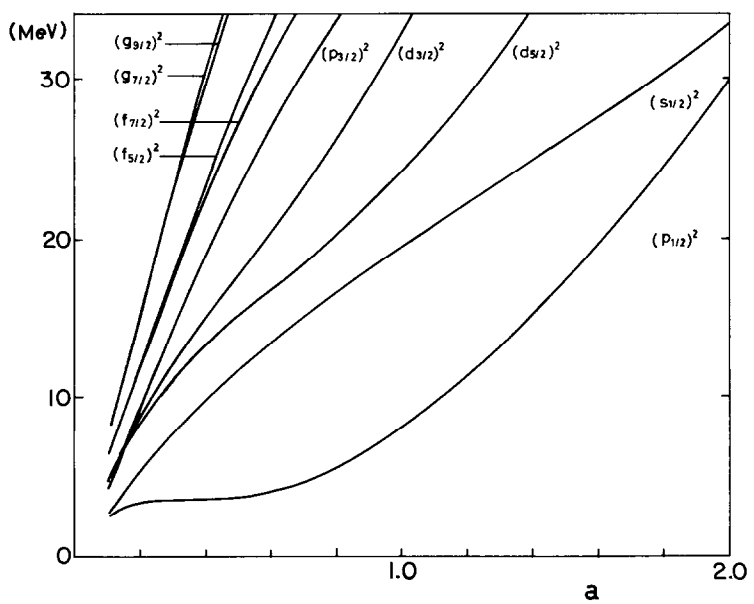

Fig. 3. The energy of ^{11}Li from ^{9}Li+n+n as a function of the parameter a for the two-neutron configurations with seniority zero.

The discrete set of a included are chosen as follows:

$$a = 0.24 \times 10^{(i-1)/9} \qquad (i = 1, 2, \ldots, 10) \quad \text{for } p_{1/2},$$

$$a = 0.24 \times (\tfrac{25}{3})^{(i-1)/4} \qquad (i = 1, 2, \ldots, 5) \quad \text{for } s_{1/2},$$

$$a = 0.24 \times 6.25^{(i-1)/3} \qquad (i = 1, 2, \ldots, 4) \quad \text{otherwise}.$$

Thus the number of the basis wave functions is $\frac{1}{2} \times 10 \times 11 = 55$ in case (1) and 140 in case (4). Table 1 lists the calculated energy for cases (1)-(4). Also shown are the contribution of each term of the hamiltonian. It is impressive that the energy gain due to the quite extensive configuration mixing is only 0.23 MeV. The calculated energy of case (4) is still higher than the observed one by about 1.4 MeV. We see that the configuration mixing increases the two-neutron interaction matrix elements but does not play a very effective role in reaching the required value of about -1.8 MeV. The ground state wave function is dominated by the $(p_{1/2})^2_{J=0}$ configuration. To estimate the importance of states other than $(j)^2_{J=0}$ we have compared two cases (2) and (2'), where case (2)' includes the following states

(2') $(p_{1/2})^2_{J=0}$, $(s_{1/2})^2_{J=0}$, $(d_{5/2})^2_{J=0}$, $(d_{3/2})^2_{J=0}$, $(p_{1/2}p_{3/2})_{J=2}$, $(p_{1/2}f_{5/2})_{J=2}$, $(s_{1/2}d_{5/2})_{J=2}$, $(s_{1/2}d_{3/2})_{J=2}$.

The result is also shown in table 1 and confirms that there is essentially no difference between cases (2) and (2'). The binding energies of the Li isotopes calculated in the $(0+2)\hbar\omega$ shell-model space [4]) show that there is a good agreement between theory and experiment up to ^{10}Li but the ^{11}Li energy is predicted to be higher than the observed one by about 1.7 MeV.

The HN potential acting between the two valence neutrons has a repulsive part at a short distance and thus requires small amplitudes in the short distance behavior of the relative wave function of the two neutrons in order to gain energy. This damping may not be fully taken into account in the present model because our basis states are given on the basis of the independent particle picture. This discussion is plausible when we compare $\langle v_{12} \rangle = -0.84$ MeV of case (4) to the value obtained in case of the pure n+n system, -1.7 MeV (see sect. 2.3). To see this point further

TABLE 1

The energy of ^{11}Li from ^{9}Li+n+n and the contribution of each term of the hamiltonian in units of MeV. The experimental energy is -0.20 MeV. The HN no. 1 potential is used as the central part acting between the two valence neutrons. See the text for cases (1) to (4) and case (2')

Case	E	$\langle h_1 + h_2 \rangle$	$\langle v_{12} \rangle$	$\langle \frac{1}{10m} \boldsymbol{p}_1 \cdot \boldsymbol{p}_2 \rangle$
(1)	1.44	1.77	−0.33	0.0
(2)	1.30	1.97	−0.59	−0.08
(3)	1.24	2.12	−0.77	−0.11
(4)	1.21	2.17	−0.84	−0.12
(2)'	1.29	1.97	−0.59	−0.09

we have repeated the calculation using the Volkov potential which has no repulsion at short distance. The results of the calculation are shown in table 2. As expected increasing the configuration mixing lowers the energy compared to the HN potential and gains more two-neutron interaction energy. However, the energy is still deficient by about 1 MeV. The percentage of the $(s_{1/2})^2_{J=0}$ configuration grows to about 5% but the $(p_{1/2})^2$ configuration still occupies about 90% of the norm of the wave function.

3.2. RADIUS AND DENSITY DISTRIBUTION

The matter mean square radius of ^{11}Li is related to that of ^{9}Li according to the formula

$$[R^{\mathrm{M}}_{\mathrm{r.m.s.}}(^{11}\mathrm{Li})]^2 = \frac{9}{11}[R^{\mathrm{M}}_{\mathrm{r.m.s.}}(^{9}\mathrm{Li})]^2 + \frac{10}{11^2}\frac{10}{9}(\xi_1^2+\xi_2^2) - \frac{2}{11^2}\frac{10}{9}\boldsymbol{\xi}_1\cdot\boldsymbol{\xi}_2 . \tag{13}$$

Similarly it is possible to relate the proton and neutron mean square radii of ^{11}Li to those of ^{9}Li as follows

$$[R^{\mathrm{p}}_{\mathrm{r.m.s.}}(^{11}\mathrm{Li})]^2 = [R^{\mathrm{p}}_{\mathrm{r.m.s.}}(^{9}\mathrm{Li})]^2 + \frac{1}{11^2}\frac{10}{9}(\boldsymbol{\xi}_1+\boldsymbol{\xi}_2)^2 ,$$

$$[R^{\mathrm{n}}_{\mathrm{r.m.s.}}(^{11}\mathrm{Li})]^2 = \frac{6}{8}[R^{\mathrm{n}}_{\mathrm{r.m.s.}}(^{9}\mathrm{Li})]^2 + \frac{1}{8}\frac{10}{9}(\xi_1^2+\xi_2^2) + \frac{1}{11}\left(\frac{1}{11}-\frac{2}{8}\right)\frac{10}{9}(\boldsymbol{\xi}_1+\boldsymbol{\xi}_2)^2 . \tag{14}$$

To arrive at eq. (14) we omit the cross terms, linear in both $\boldsymbol{\xi}_i$ and the internal coordinates of ^{9}Li. We replace the proton and neutron radii of ^{9}Li with the values deduced from the analysis of the interaction cross section [1]), i.e., $R^{\mathrm{p}}_{\mathrm{r.m.s.}}(^{9}\mathrm{Li}) = 2.18 \pm 0.02$ fm, $R^{\mathrm{n}}_{\mathrm{r.m.s.}}(^{9}\mathrm{Li}) = 2.39 \pm 0.02$ fm. It is also easy to evaluate the expectation values of the mean square distance between the valence neutron and the ^{9}Li core, $D^2_{\mathrm{r.m.s.}}$, and the mean square distance between the two valence neutrons, $d^2_{\mathrm{r.m.s.}}$. Table 3 lists the values of these quantities calculated by using the wave functions obtained with the HN potential in cases (1)–(4). The calculated value of the matter radius $R^{\mathrm{M}}_{\mathrm{r.m.s.}}(^{11}\mathrm{Li})$ is in excellent agreement with the experimental value. Our result is quite

TABLE 2

The energy of ^{11}Li from ^{9}Li+n+n and the contribution of each term of the hamiltonian in units of MeV in case of the Volkov no. 2 potential. See the caption of table 1

Case	E	$\langle h_1+h_2\rangle$	$\langle v_{12}\rangle$	$\langle \frac{1}{10m}\boldsymbol{p}\cdot\boldsymbol{p}_2\rangle$
(1)	1.35	1.78	−0.43	0.0
(2)	1.09	2.19	−0.98	−0.11
(3)	0.93	2.60	−1.49	−0.19
(4)	0.87	2.79	−1.70	−0.21

TABLE 3

Root mean square radii of ^{11}Li in units of fm. See the text for their definitions

	$R^{M}_{r.m.s.}$	$R^{p}_{r.m.s.}$	$R^{n}_{r.m.s.}$	$D_{r.m.s.}$	$d_{r.m.s.}$
Present case: (1)	3.28	2.32	3.58	6.21	8.78
(2)	3.21	2.33	3.49	6.01	8.01
(3)	3.20	2.33	3.47	5.97	7.79
(4)	3.19	2.33	3.46	5.97	7.73
Ref. [4])	2.81	2.50	2.92		
Ref. [5]) (SKV)	2.61	2.24	2.74		
Ref. [6])	2.846	2.153	3.066		
Ref. [1]) (exp.)	3.16 ± 0.11	(2.88 ± 0.11) [a])	(3.21 ± 0.17) [a])		

[a]) The experimental values of the proton and neutron radii of ^{11}Li are subject to question (I. Tanihata, private communication).

satisfactory compared to the values of refs. [4–6]). Although there is a difference between theory and experiment for the proton and neutron radii, we note that the experimental values are deduced by assuming simple harmonic-oscillator wave functions in the common well and do not properly reflect the situation where the two valence neutrons spread out to a far distance. It is dangerous to deduce both the proton and neutron radii from the interaction cross sections only. The values of $D_{r.m.s.}$ and $d_{r.m.s.}$ indicate that the configuration mixing tends to decrease both distances to form a compact system. The value of $R^{M}_{r.m.s.}(^{11}\mathrm{Li})$ in case (4) with the Volkov no. 2 potential is 3.11 fm.

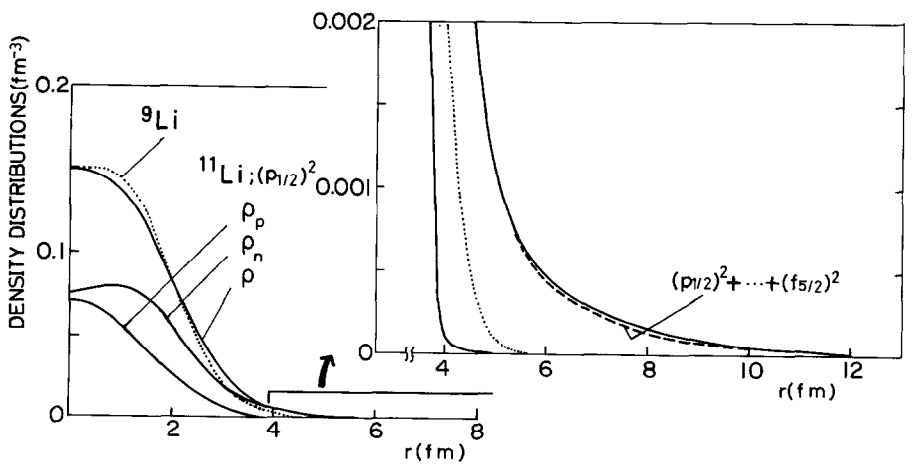

Fig. 4. The density distributions of ^{11}Li. As the configuration mixing does not yield a sizable difference, the distribution for the $(p_{1/2})^2_{J=0}$ configuration (case (1)) is drawn. The nucleon density distribution of ^{9}Li is shown by the dotted curve for the sake of comparison. The tail parts of the distributions enlarged by 100 are shown in the right figure, where the neutron density coincides with the nucleon density.

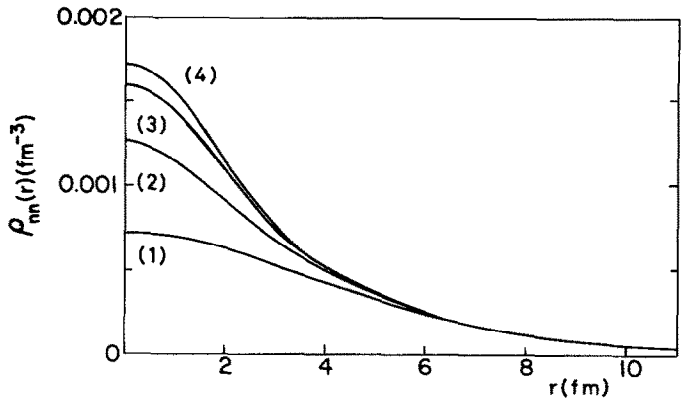

Fig. 5. The density distribution of the relative wave functions between the two valence neutrons. See the text for cases (1)-(4).

Fig. 4 displays the density distributions of ^{11}Li averaged over the z-component of the ^{11}Li spin. Both the proton and neutron distributions are also shown separately. Compared to the nucleon density distribution of ^{9}Li shown by the dotted curve, the nucleon density distribution of ^{11}Li has a slower fall-off and a long-ranged tail with very low density. The proton density is concentrated in the inner region while the neutron density spreads over to a large distance. It has recently been suggested [16] that this asymmetry of the proton and neutron densities seen in very neutron-rich nuclei leads to low-frequency dipole vibrations where the excess neutrons vibrate against the core. We note that the effect of the configuration mixing is hardly seen except for the extremely large distances in this figure. The dashed curve in the expanded figure is the nucleon density obtained with the wave function of case (3). Fig. 5 shows the configuration mixing dependence of the density distribution, $\rho(|\boldsymbol{r}_1-\boldsymbol{r}_2|)$, of the relative wave functions between the two valence neutrons. It is seen that the configuration mixing plays the role of increasing this density at small distances.

4. Summary and discussion

We have studied the structure of ^{11}Li in the cluster-orbital shell model for the system of ^{9}Li+n+n. The ^{9}Li nucleus is described with a $0\hbar\omega$ shell model wave function. The ^{9}Li-n potential and the central part of the two-neutron interaction are determined consistently with the available data. The valence neutrons are distributed among the single-particle orbits of $p_{1/2}$, $s_{1/2}$, $d_{5/2}$, $d_{3/2}$, $p_{3/2}$, $f_{7/2}$, $f_{5/2}$, $g_{9/2}$ and $g_{7/2}$. The radial part of each orbit consists of a superposition of several gaussian functions and thus enables us to describe very extended radial motion. Our calculation is entirely free from the spurious center-of-mass motion. The main results are summarized as follows:

(i) The configuration mixing of the large bases for the valence neutrons serves to gain energy but the calculated energy of ^{11}Li is still 1–1.4 MeV higher than the experimental value.

(ii) The interaction energy between the two valence neutrons increases as the number of the basis functions increases. The extent to which it increases is dependent on the radial dependence of the two-neutron interaction at short distance.

(iii) The $(p_{1/2})^2_{J=0}$ configuration is the dominant component of the ground state wave function. The contribution of wave functions with non-zero seniority is negligibly small. This property leads us to the expectation that both the magnetic and quadrupole moments of ^{11}Li are almost the same as those of ^{9}Li. A recent measurement [10]) of the ^{11}Li magnetic moment (3.67 n.m.) confirms this expectation. A measurement of the quadrupole moment will be very useful as a test of models of ^{11}Li.

(iv) The experimental value of the matter root mean square radius is reproduced quite well by the present model. The root mean square distance between ^{9}Li and the valence neutron is about 6 fm.

(v) Compared to ^{9}Li, the density distribution of ^{11}Li has a slower fall-off and a much longer tail. There is a large difference between the proton and neutron density distributions. The density distribution of the relative wave function between the two valence neutrons becomes more peaked at short distance as the configuration mixing increases. The results (iv) and (v) clarify what is meant by the neutron halo.

As stated in (i), the binding mechanism of ^{11}Li is not fully accounted for by the present model. The result (ii) indicates the importance of taking full account of the correlation energy between the two valence neutrons for binding the ^{9}Li+n+n system. Let us ask the question of how well the di-neutron correlation can be described with the configuration mixing of the wave functions used in this paper. The angular dependence of the $(l_j)^2_{J=0}$ wave function in the singlet-even state of the two neutrons is given by the Legendre polynomial $P_l(\cos\theta)$, where θ is the angle between the two coordinates ξ_1 and ξ_2. As $P_l(\cos\theta)$ is peaked at $\theta \lesssim 1/l$, the order of the two-neutron distance is $d \approx R/l$, where R is the distance between ^{9}Li and the center-of-mass of the two neutrons. Since R is about 5–6 fm and the maximum of l is 4 in the present calculation, the two-neutron relative wave function is spread at least to about 1.2 fm. Thus the present model space may not be enough to describe such wave functions as the short ranged repulsive force requires. If we had to take into account the short range correlation up to the order of 0.5 fm, the maximum l needed in the calculation would be at least about 10.

The lack of binding energy by 1–1.4 MeV seems to indicate the insufficiency of the description of the di-neutron correlation with the present model. If this is the case, it may be necessary to include explicitly a configuration of the di-neutron cluster moving around the ^{9}Li core as suggested in ref. [17]). In any case, it is desirable, although challenging, to use more realistic interactions such as the Paris potential as the interaction between the two valence neutrons.

The authors thank Drs. K. Ikeda, T. Kaneko and K. Yabana for useful discussions and suggestions and Dr. I. Tanihata for his interest and encouragement. They are also grateful to Mr. T. Tamura for his collaboration at the early stage of this work. Thanks are due to Dr. K.T. Hecht for his careful reading of the manuscript. The manuscript has been completed while one of the authors (Y.S.) stays at the University of Michigan. He expresses his hearty gratitude to Dr. Hecht for the generosity and hospitality extended to him.

References

1) I. Tanihata *et al.*, Phys. Rev. Lett. **55** (1985) 2676; Phys. Lett. **B160** (1985) 380; Preprint RIKEN-AF-NP-60 (1987)
I. Tanihata, Nucl. Phys. **A478** (1988) 795c; **A488** (1988) 113c
2) T. Kobayashi *et al.*, Phys. Rev. Lett. **60** (1988) 2599
3) P.G. Hansen and B. Jonson, Europhys. Lett. **4** (1987) 409
4) N.A.F.M. Poppelier, L.D. Wood and P.W.M. Glaudemans, Phys. Lett. **B157** (1985) 120; N.A.F.M. Poppelier, J.H. de Vries, A.A. Wolters and P.W.M. Glaudemans, in AIP Conf. Proc. **164** (1988) 334
5) H. Sato and Y. Okuhara, Phys. Lett. **B162** (1985) 217; Phys. Rev. **C34** (1986) 2171
6) G.F. Bertsch, B.A. Brown and H. Sagawa, Phys. Rev. **C39** (1989) 1154
7) Y. Suzuki and K. Ikeda, Phys. Rev. **C38** (1988) 410
8) Y. Suzuki and J.-J. Wang, Phys. Rev. **C41** (1990) 736
9) F.D. Correll, L. Madansky, R.A. Hardekopf and J.W. Sunier, Phys. Rev. **C28** (1983) 862
10) E. Arnold *et al.*, Phys. Lett. **B197** (1987) 311; Z. Phys. **A331** (1988) 295
11) Y. Suzuki, Nucl. Phys. **A405** (1983) 40; Proc. Fifth Int. Conf. on clustering aspects in nuclear and subnuclear systems, Kyoto (1988), ed. K. Ikeda, K. Katori and Y. Suzuki, J. Phys. Soc. Jpn. **58** Suppl. (1989) 129
12) H. Furutani *et al.*, Prog. Theor. Phys. Suppl. **68** (1980) 193
13) A.G.M. van Hees and P.W.M. Glaudemans, Z. Phys. **A315** (1984) 223
14) F.C. Barker and G.T. Hickey, J. of Phys. **G3** (1977) L23
15) A. Volkov, Nucl. Phys. **74** (1965) 33
16) H. Sato, Y. Suzuki and K. Ikeda, Proc. Int. Symp. on heavy ion physics and nuclear astrophysical problems, Tokyo, 1988, ed. S. Kubono, M. Ishihara and T. Nomura (World Scientific, Singapore, 1988) p. 199
Y. Suzuki, K. Ikeda and H. Sato, Prog. Theor. Phys. **83** (1990) 180
17) A.B. Migdal, Sov. J. Nucl. Phys. **16** (1973) 238